

NEK7 mediates ESRD-associated endothelial injury by activating the NLRP3 inflammasome

Le Sun^{a,b,c,1}, Ying Ren^{a,b,c,1}, Wenping Zhu^{a,b,c,1}, Tong Ni^d,
Songming Huang^{a,b,c}, Aihua Zhang^{a,b,c}, Yue Zhang^{a,b,c}, Hu Hua^{a,b,c,*},
Zhanjun Jia^{a,b,c,*}, Zhenzhen Sun^{a,b,c,*}

^a Department of Nephrology, Children's Hospital of Nanjing Medical University, Guangzhou Road #72, Nanjing 210008, PR China

^b Nanjing Key Laboratory of Pediatrics, Children's Hospital of Nanjing Medical University, Guangzhou Road #72, Nanjing 210008, PR China

^c Jiangsu Key Laboratory of Early Development and Chronic Diseases Prevention in Children, Nanjing Medical University, Nanjing 210029, PR China

^d Department of Endocrinology, Affiliated Changzhou Children's Hospital of Nantong University, Changzhou 213003, PR China

ARTICLE INFO

Editor name: Dr. Hajo Haase

Keywords:

Uremia

Indoxyl sulfate

NEK7

NLRP3 inflammasome

Endothelial injury

ABSTRACT

Cardiovascular disease (CVD) is reported to closely associate with the high mortality in patients with end-stage renal disease (ESRD), and endothelial damage induced by accumulated uremic toxins (mostly studied indoxyl sulfate [IS]) is the key pathological process, whose pathogenesis and therapeutic strategies remain incompletely understood. NIMA-related kinase 7 (NEK7) has been recognized as a novel mediator for NLRP3 inflammasome activation, which plays a crucial part in causing vascular endothelial injury. Here, we explored the potential functions and fundamental mechanisms of NEK7-mediated NLRP3 inflammasome activation in IS-induced endothelial injury. Expression of the NLRP3 inflammasome and its activation were markedly increased in IS-administered endothelium both in vivo and in vitro. Silencing NEK7, NLRP3, or caspase 1 significantly inhibited NLRP3 inflammasome activation, thereby alleviating IS-induced endothelial injury, as indicated by reduced inflammation and apoptosis in mouse arterial endothelial cells (MAECs). Furthermore, impaired endothelium in the aortas of both five-sixths nephrectomy mice and IS-injected mice with activated NLRP3 inflammasome, was either restored when conditional knockdown of NEK7 in endothelial cells or amplified upon NEK7 over-expression via hydrodynamic tail vein injection. Together, we validate that NEK7 promotes IS-induced endothelial injury by activating the NLRP3 inflammasome, which not only sheds lights on the underlying mechanisms of IS-mediated endothelial injury in ESRD, but also provides potential pharmacological target for the therapy of ESRD-related CVD.

1. Introduction

Chronic kidney disease (CKD) has drawn great concern in the world for a long time due to its high morbidity, costly treatment, and severe complications [1–5]. In the setting of stage 4 chronic kidney disease (ESRD), cardiovascular disease (CVD) is the most common cause of death, responsible for 50 % of all deaths [6–11]. Effective therapies are needed in light of the alarmingly high prevalence of CVD among ESRD patients, which necessitates a deeper comprehension of the pathogenic

processes causing ESRD-related CVD.

In ESRD, impaired renal function gives rise to accumulated uremic toxins, among which protein-bound uremic toxins are particularly challenging for conventional dialysis to eliminate due to their high affinity for albumin [12]. Among various uremic toxins, indoxyl sulfate (IS) has been mostly investigated. Indoxyl sulfate is a protein-bound uremic toxin, and it originates from dietary tryptophan and usually achieves high clearance in healthy kidneys through tubular secretion via organic anion transporters [13,14]. Evidence has indicated that IS is

Abbreviations: ESRD, end-stage renal disease;; CVD, cardiovascular disease; IS, indoxyl sulfate; NEK7, NIMA-related kinase 7; 5/6Nx, five-sixths nephrectomy; Cr, serum creatinine; BUN, blood urea nitrogen..

* Corresponding authors at: Nanjing Key Laboratory of Pediatrics, Children's Hospital of Nanjing Medical University, 72 Guangzhou Road, Nanjing 210008, PR China.

E-mail addresses: gavinhua@njmu.edu.cn (H. Hua), jiazhazhanjun72@njmu.edu.cn (Z. Jia), sunzz2018@njmu.edu.cn (Z. Sun).

¹ These authors contributed equally to this work.

<https://doi.org/10.1016/j.intimp.2025.115236>

Received 6 February 2025; Received in revised form 1 July 2025; Accepted 11 July 2025

Available online 21 July 2025

1567-5769/© 2025 Elsevier B.V. All rights are reserved, including those for text and data mining, AI training, and similar technologies.

markedly increased in the serum of patients with uremia compared with healthy individuals [15,16], and continuous challenge with IS leads to damage to the vascular endothelium [17], that is demonstrated by the induction of endothelial oxidative stress [18] and microparticles [19], as well as endothelial apoptosis and the retardation of endothelial proliferation [20]. Clinical data have also indicated that IS acts independently to pose a threat to the lives of patients with CVD in the setting of ESRD [21]. Several molecular mechanisms are involved in IS-induced endothelial injury, including phosphorylation of the p38–MAPK pathway [22,23], upregulation of NADPH oxidase activity [24], and down-regulation of eNOS expression [25]. However, few effective targets have been identified; thus, in-depth studies are urgently needed to find novel mechanistic mechanisms for endothelial impairment under IS challenge.

A number of investigations have supported a close correlation between the impairment of vascular endothelium and the activation of the NLRP3 inflammasome [26–34]. A previous report concluded that the toxic uremic metabolite trimethylamine-N-oxide (TMAO) induced the activation of the NLRP3 inflammasome via downregulation of sirtuin 3, amplifying inflammation and endothelial dysfunction [35]. The NLRP3 inflammasome reacts to certain stimulations for priming and activation, in which ASC connects NLRP3 and caspase 1, facilitates the formation of ASC specks and the activation of caspase 1, and subsequently promotes the secretion of mature IL-1 β and IL-18, driving the development of disorders associated with inflammation [36]. However, the influence of the activated NLRP3 inflammasome on IS-induced endothelium injury remains largely unknown.

As the smallest member of the NEK family, NEK7 widely distributes in various tissues which include heart, liver, kidney, and muscle [37]. It was initially reported that NEK7 mediates mitotic progression and DNA repairment and is associated with uncontrolled cell proliferation and tumorigenesis [38]. Recent reports have confirmed NEK7 could bind to NLRP3 and act to regulate NLRP3 inflammasome oligomerization and activation [39–41]. Additionally, NEK7 mutation could substantially inhibit NLRP3 inflammasome-mediated inflammation [42]. However, few investigations have revealed the contribution of NEK7-mediated NLRP3 inflammasome activation to IS-associated impairment of the vascular endothelium.

In the current study, we established uremia-related models both in vivo and in vitro. Endothelial injury, as indicated by inflammation and apoptosis, was comprehensively evaluated. The findings of this investigation offer compelling evidence that NEK7 mediates IS-induced endothelial apoptosis by activating the NLRP3 inflammasome.

2. Materials and methods

2.1. Mouse strains and animal models

All the mice used in this study were maintained under specific pathogen-free condition with controlled light (a 12 h-light/12 h-dark cycle) and temperature and free access to standard food and water in the animal care facility of Nanjing Medical University. All the procedures and animal experiments were performed complying with the ethical guidelines and approved by the Institutional Animal Care and Use Committee (IACUC-20090053, 2209063–2) of Nanjing Medical University. All mice were anesthetized by inhaling isoflurane (2 %) during the process of five-sixths nephrectomy (5/6Nx) and Sham operation. At the end of each model, all the mice were euthanized under isoflurane (2 %) inhalation followed by blood collection from inferior vena cava.

C57BL/6 J mice, NEK7^{fl/fl} (B6/JNju-Nek7em1CfloX/Nju, T004197), and Tek-Cre mice (C57BL/6JGpt-Tek-iCre, T003764) were purchased from GemPharmatech Co., Ltd. (Nanjing, China). Conditional endothelial cell NEK7-knockout heterozygous mice (NEK7 cKO Het mice) were generated through the breeding of NEK7^{fl/fl} mice and Tek-Cre mice (Primer sequences for genotyping are listed in Supplemental Table 1). The reagents and primers used for genotyping were acquired following the guidelines provided by the manufacturer.

We performed 5/6Nx operation to create a simulated condition of chronic kidney failure. For C57BL/6 J mice (8 weeks old, male), they were randomly assigned to one of two groups to be subjected to sham or 5/6Nx operations. For NEK7 cKO mice (8 weeks old, male), endothelial cell NEK7 knockout heterozygotes (Het mice) and their littermates (Ctrl mice) were divided into two groups respectively: the 5/6Nx and sham groups. Both the 5/6Nx and sham operations were under anesthesia with isoflurane (2 %) inhalation and kept at a 37 °C thermostatic blanket. Briefly, to perform 5/6Nx operation, first, the upper and lower poles of the left kidney were resected via a left flank incision, and one week later, the entire right kidney was removed via a right flank incision [43]. Twelve weeks later, all the mice were euthanized under isoflurane (2 %) inhalation followed by blood collection from inferior vena cava. The thoracic aortas were removed for further analysis.

For IS-related mouse model, the C57BL/6 J mice (8 weeks old, male) were assigned into four groups ($n = 6$): Ctrl+Vehicle, NEK7 + Vehicle, Ctrl+IS, and NEK7 + IS groups. The mice were first injected with NEK7 plasmids or Ctrl plasmids (empty vector, pCDNA3.1) followed by intraperitoneal injection of IS (I3875, Sigma–Aldrich) or saline. Briefly, mouse NEK7 plasmids and control plasmids (Biogot Technology) were diluted in saline (0.9 % NaCl) at 30 μ g/ml. Each mouse was injected with 2 ml of plasmids (60 μ g) in saline through tail vein. Twenty-four hours later, an intraperitoneal injection of IS (150 mg/kg) or saline was administered to mice daily for 7 days. At the end, all mice in the four groups were euthanized under isoflurane (2 %) inhalation followed by blood collection from inferior vena cava once the experiment was finished, and the thoracic aortas were removed for further analysis.

2.2. Cell culture and treatment

Mouse aortic endothelial cells (MAECs, JNO-M0176, GuangZhou Jennio Biotech Co.,Ltd) were cultured in DMEM (C11995500BT, GIBCO) supplemented with FBS (ST30–3302, PAN) to the concentration of 10 % in a humidity-controlled incubator with 5 % CO₂ at 37 °C. To knockdown the levels of NEK7, NLRP3, or caspase 1, cells were transfected with corresponding short interfering RNA (si-NEK7, si-NLRP3, or si-caspase 1, the target sequences in Supplemental Table 2) or negative control (RIBO-biotic) delivered by Lipofectamine 2000 (11,668,019, Thermo Fisher). MAECs were then incubated in ascend concentrations (0, 250, 500, 1000 μ M) of IS (I3875, Sigma–Aldrich) with or without 5 mM adenosine triphosphate (ATP, A2383, Sigma–Aldrich) for 24 h.

2.3. Immunohistochemistry (IHC) and immunofluorescence (IF) staining

Fresh aortas were processed from dehydration to paraffin-embedding, made from 2 to 3- mm small segments into 4- μ m sections for the subsequent dewaxing and antigen retrieval.

For IHC staining, the aorta tissue slides were blocked in 3 % hydrogen peroxide (PV-9000, ZSGB-BIO) for 20 min, in QuickBlock blocking buffer (P0260, Beyotime) for 1 h, and in immunol staining dilution buffer (P0103, Beyotime) with anti-rabbit cleaved caspase 3 (1:400 dilution, 9661, CST), anti-rabbit IL-1 β (1:100 dilution, bs-6319R, Bioss) or anti-rabbit NEK7 (1:50 dilution, bs-7758R, Bioss) primary antibody overnight at 4 °C. The slides were processed by the two-step test kit (PV-9000, ZSGB-BIO) in the following day as instructed. Then, a DAB kit (ZLI-9018, ZSGB-BIO) was used to visualize the positive areas on the slides. The staining density was quantified using ImageJ.

For IF staining, following the incubation of the aorta tissue slides with anti-rabbit ASC (1:200 dilution, AL177, AdipoGen) primary antibody overnight at 4 °C was the incubation with Alexa Fluor 488 marked goat anti-rabbit IgG (H + L) (A0423, Beyotime) secondary antibody for 1.5 h at room temperature. The stain used on the nuclei was DAPI (P0131, Beyotime). For staining of NLRP3-ASC colocalization, anti-rabbit NLRP3 (1:50 dilution, 19771–1-AP, proteintech) and anti-rabbit ASC (1:200 dilution, AL177, AdipoGen) primary antibody combined with a tyramide signal amplification (TSA) staining kit (YB005,

YOIBIO, Shanghai, China) were used. For capturing the images, a Leica confocal microscope (DMi8) was used. The cells were planted on cell culture slides in preparation for IF labeling. Following treatment, 4 % paraformaldehyde was utilized for fixation for 20 min, 0.2 % Triton X-100 (P0096, Beyotime) was utilized for permeabilization for 15 min, and QuickBlock blocking buffer (P0260, Beyotime) was utilized for blockage for 1 h. The following steps were the same as those described for the paraffin-embedded aortic sections. The images were captured using a Zeiss confocal microscope (LSM710). The staining density was quantified using ImageJ.

2.4. Caspase 1 activity analysis

A Caspase 1/ICE colorimetric assay kit (K111–100, BioVision) was utilized to determine the activity of caspase 1. According to the guidelines, we collected cell lysates and measured the protein concentrations. Then, the proteins were resuspended in chilled cell lysis buffer and further incubated in YVAD-pNA for 1–2 h at 37 °C. Microplates were added with samples to be tested, and 405 nm wavelength was used to detect the results.

2.5. ELISA

An ELISA kit (1,210,122, Dakewe) was utilized to quantitatively assess the concentration of IL-1 β contained in the medium of MAECs treated as established. As demonstrated by the manufacturer's instruction, 100 μ l of each sample were used for test. This was followed by the addition of 50 μ l of the Biotinylated antibody working solution to each well, and the plate was incubated at 37 °C for 90 min. Afterward, the contents of the wells were aspirated and washed 4 times before the addition of 100 μ l/well of the Streptavidin-HRP working solution. The plate was then incubated again at 37 °C for 30 min. Following another round of 4 times of washing, 100 μ l/well of the TMB working solution was added. The plate was incubated at 37 °C for 5 to 20 min, after which 100 μ l/well of Stop solution was promptly added to stop the reaction. The final absorbance was measured at 450 nm.

2.6. FITC annexin V assay

As for the assessment of cell death, an FITC Annexin V kit (556,547, BD) was used. MAECs were planted in a twelve-well plate (TCP011012, BIOFIL) at the concentration of $0.5\text{--}1 \times 10^5$ cells per well. After treatment, MAECs and their supernatants were collected in 1.5 ml centrifuge tubes, rinsed in PBS, and resuspended in binding buffer with FITC-Annexin V and PI for 15 min in the absence of light at ambient temperature. The cells were analyzed by flow cytometry (Cytoflex) immediately at the end of the staining.

2.7. Western blot analysis

To extract the total proteins, MAECs and mouse aortic tissues were subjected to RIPA lysis buffer (A0181, Beyotime), which was further posted on ice for 20 min and centrifugated at 4 °C for 20 min at 13,800 g (12,000 rpm). Then the supernatants were collected for further measurement of protein concentrations. Subsequently, proteins were denatured in SDS-PAGE loading buffer (P0015L, Beyotime) at 100 °C for 5 min. A standard western blot analysis was then conducted. In brief, we use 10 % polyacrylamide separating gels to separate the protein samples and polyvinylidene difluoride membranes to electroblot them. Following the blockage with 5 % nonfat milk at ambient temperature for 1 h was the incubation with the following primary antibodies overnight at 4 °C: anti-rabbit NEK7 (1:1000 dilution, ab133514, abcam), anti-rabbit NLRP3 (1:1000 dilution, 9771–1-AP, proteintech), anti-rabbit Casp1/p10/p12 (1:1000 dilution, ab179515, abcam), anti-rabbit caspase 3 (1:1000 dilution, 14220, CST), anti-rabbit gasdermin D (1:1000 dilution, ab219800, abcam), anti-rabbit cleaved gasdermin D (1:1000

dilution, 36425, CST), anti-rabbit β -actin (1:2000 dilution, 20536–1-AP, proteintech), anti-mouse α -tubulin (1:2000 dilution, 66031–1-Ig, proteintech). HRP-labeled goat anti-rabbit (1:2000 dilution, A0208, Beyotime) and anti-mouse (1:2000 dilution, A0216, Beyotime) antibodies were used as secondary antibodies in the next day. The results were then visualized on a BIO-RAD ChemiDoc XRS+, and protein intensity was analyzed using ImageJ.

2.8. Quantitative real-time PCR (qRT-PCR)

To distill the total RNA, MAECs and mouse aortic tissues were subjected to RNAiso Plus (9109, Takara). 2000 ng of RNA was then reversed to cDNA using a reverse transcriptase (2641 A, Takara). To determine the mRNA expression levels, qRT-PCR was performed in a 96-well QuantStudio 3 Real-time PCR System (Applied Biosystems). The $2^{-\Delta\Delta C_t}$ approach was employed to determine the relative alterations in mRNA levels. A specific list of PCR primers was outlined in Supplemental Table 3.

2.9. Statistical analysis

In this study, we used GraphPad prism (10.0) to analyze the data and presented it as mean \pm SEM. The statistical importance between groups was assessed by an unpaired Student's *t*-test or a one-way ANOVA by SPSS (19.0). *P* < 0.05 was considered statistically significant.

3. Results

3.1. IS increases the expression of NEK7 and NLRP3 inflammasome components in MAECs

First, we examined the role of IS in the expression of NEK7, NLRP3, and caspase 1. MAECs were incubated in serum-free medium with different concentrations (0, 250, 500, and 1000 μ M) of IS for 24 h, and by Western blot and qRT-PCR analysis, we observed that IS treatment significantly increased the protein and the mRNA levels of NEK7, NLRP3, and caspase 1 in MAECs (Fig. 1A–D, F–H), whereas there were no evident changes in IL-1 β mRNA levels (Fig. 1I) and caspase 1 activity (Fig. 1A, E, J). In general, the activation of the NLRP3 inflammasome occurs in two steps, which contains signal 1-induced priming and signal 2-facilitated assembly and activation [44–52]. These results suggested that IS upregulated NEK7/NLRP3/caspase 1 expression in MAECs, possibly participating in the priming of the NLRP3 inflammasome, which is a crucial initial stage for the activation of the NLRP3 inflammasome [53,54].

3.2. IS and ATP act in a synergic manner to induce NLRP3 inflammasome activation in MAECs

To further investigate the impact of IS on the activation of the NLRP3 inflammasome, we subjected MAECs to IS in combination with ATP, a classic stimulator in the second phase of NLRP3 inflammasome activation. MAECs were treated with Ctrl, ATP (5 mM), IS (1000 μ M), and a combination of IS (1000 μ M) and ATP (5 mM). Consistently, IS notably upregulated NEK7, NLRP3, and caspase 1 expressions at both protein and mRNA levels (Fig. 2A–D, F–H). However, no distinct changes were observed in the levels of NEK7 and NLRP3 between the two groups in which MAECs were exposed to IS with or without ATP (Fig. 2A–D, F–G). Indeed, ATP administration not only promoted the cleavage of caspase 1 stimulated by IS (Fig. 2A, E), but also elevated IS-induced caspase 1 and IL-1 β transcript levels (Fig. 2H–I). Furthermore, ASC-immunofluorescence staining, a caspase 1 activity assay, and ELISA were performed to evaluate ASC speck formation, caspase 1 activity, and IL-1 β release, respectively. We observed that ATP promoted the activation of the NLRP3 inflammasome primed by IS, as evidenced by the elevation of ASC speck formation (Fig. 2J–K), enhanced caspase 1

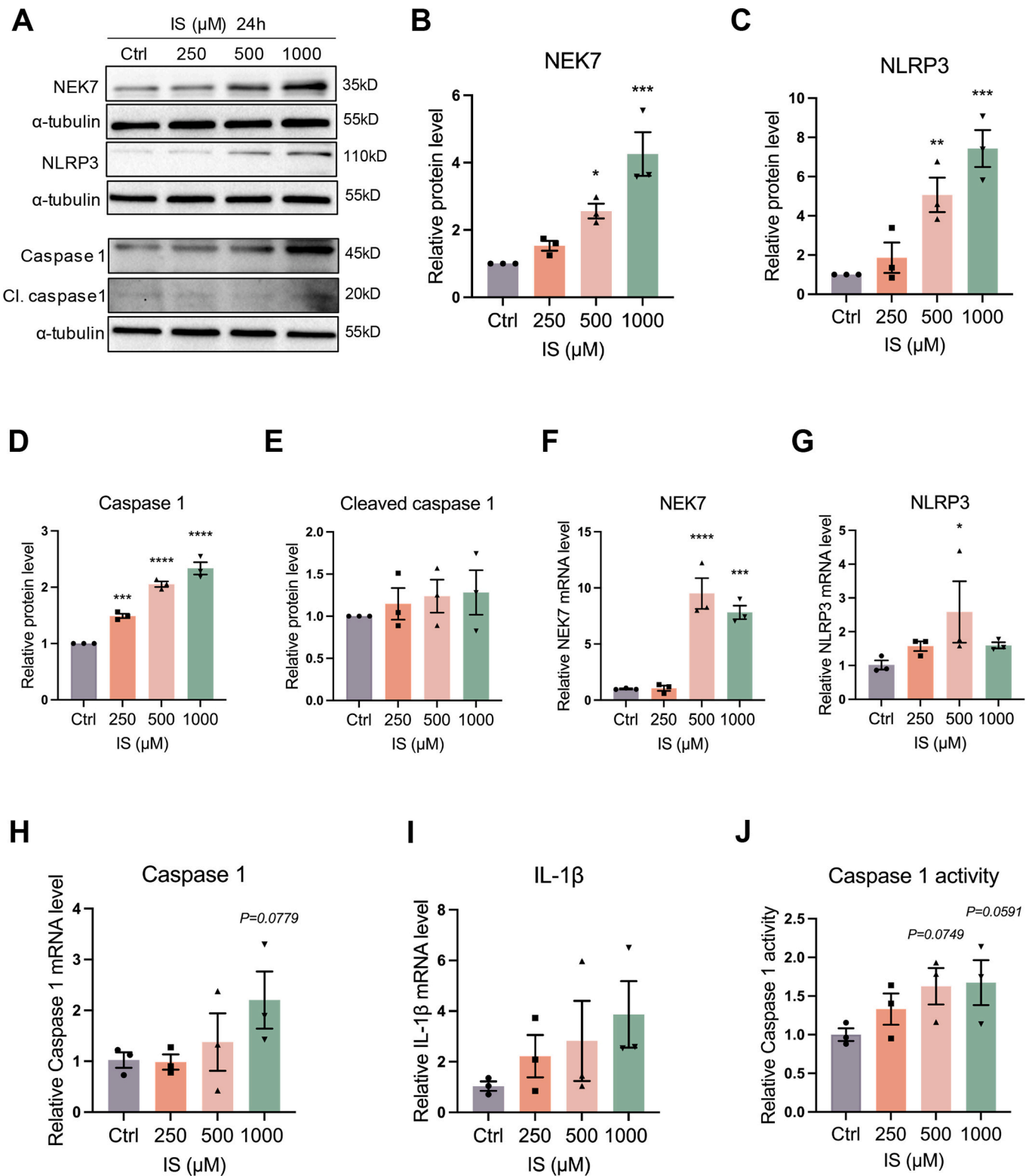


Fig. 1. IS increases the expression of NEK7 and NLRP3 inflammasome components in MAECs.

(A–E) Western blot analysis of NEK7, NLRP3, caspase 1 and cleaved caspase 1 in MAECs treated with IS (250, 500, and 1000 μ M) for 24 h, $n = 3$. (F–I) Transcript levels of NEK7, NLRP3, caspase 1, and IL-1 β in MAECs from each group, $n = 3$. (J) Caspase 1 activity in MAECs under the dose course of IS, as examined by a Caspase 1/ICE colorimetric assay kit, $n = 3$. One-way ANOVA followed by Benjamini's multiple comparisons test were used to determine the p -values. * $P < 0.05$, ** $P < 0.01$, *** $P < 0.001$, **** $P < 0.0001$.

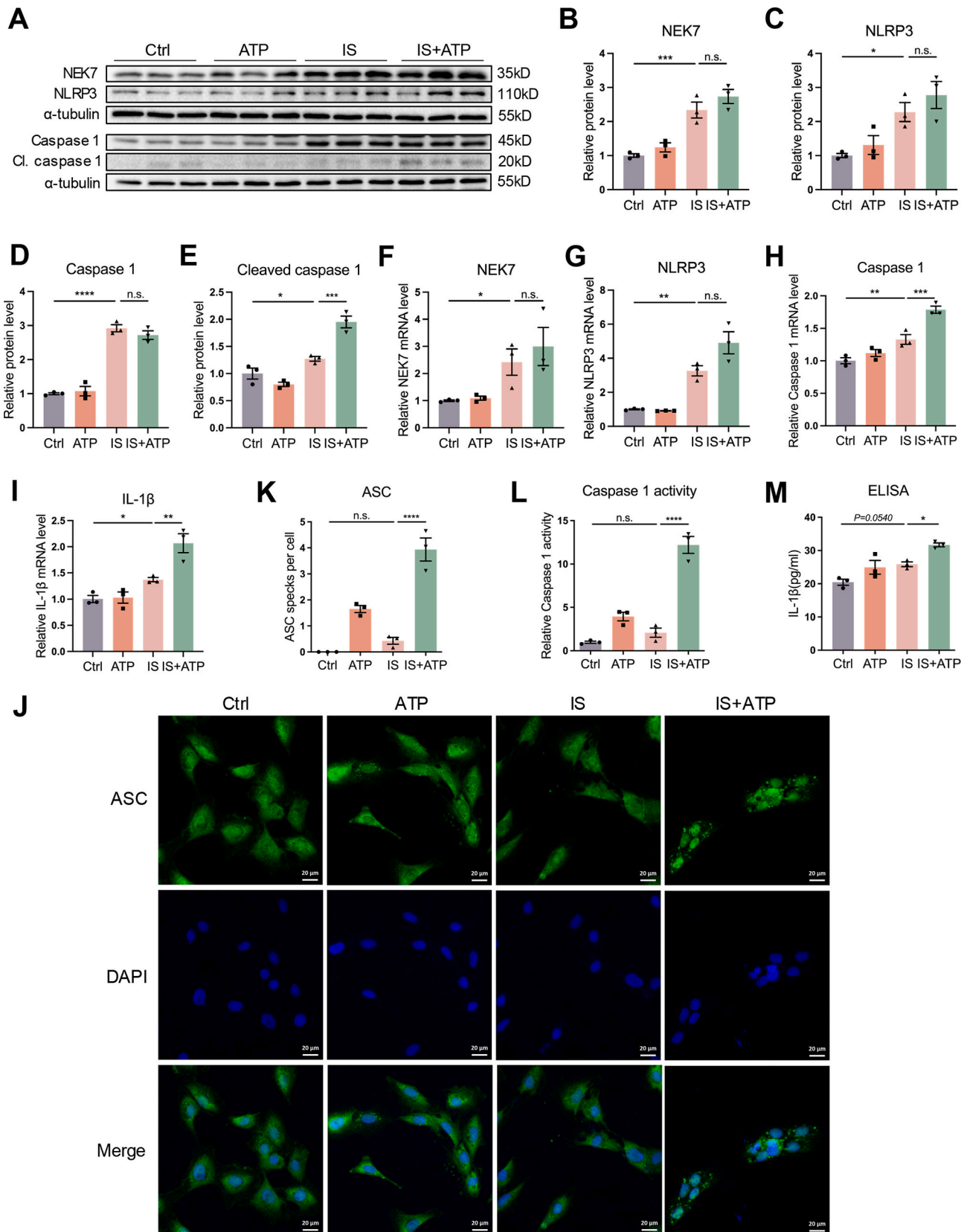


Fig. 2. IS and ATP act in a synergistic manner to induce NLRP3 inflammasome activation in MAECs.

(A–E) Western blot analysis of NEK7, NLRP3, caspase 1 and cleaved caspase 1 in MAECs following 24 h of treatment of the Ctrl, 5 mM ATP, 1000 μ M IS, and 1000 μ M IS + 5 mM ATP groups, $n = 3$. (F–I) Transcript levels of NEK7, NLRP3, caspase 1, and IL-1 β in MAECs exposed to 1000 μ M IS with or without 5 mM ATP for 24 h, $n = 3$. The activation status of the NLRP3 inflammasome from each group of MAECs, characterized according to the formation of ASC specks by immunofluorescence (J–K), the activity of caspase 1 by a Caspase 1/ICE colorimetric assay kit (L), and the secretion of IL-1 β by ELISA (M), $n = 3$. One-way ANOVA followed by Benjamini's multiple comparisons test were used to determine the p-values. * $P < 0.05$, ** $P < 0.01$, *** $P < 0.001$, **** $P < 0.0001$.

activity (Fig. 2L), and increased IL-1 β release (Fig. 2M). Taken together, these findings demonstrated that IS further triggered NLRP3 inflammasome activation by the addition of ATP in MAECs.

3.3. NEK7 silencing attenuates inflammation in MAECs induced by IS and ATP

Next, we determined the levels of other inflammatory cytokines and observed significant upregulations of IL-6 and TNF- α mRNA expression

in MAECs administered various concentrations of IS (Fig. 3A–B). Furthermore, upon exposing MAECs to IS in combination with ATP (IS+ATP), we observed marked increases in the levels of IL-6 and TNF- α compared with the IS alone group (Fig. 3C–D). To further determine whether inhibition of NEK7 could impede IS+ATP-induced inflammation in MAECs, NEK7 siRNA was used to transfect the cells, which were subsequently exposed to IS+ATP treatment. Notably, compared with the control, NEK7 deficiency downregulated IL-6 and IL-1 β transcript levels induced by IS+ATP (Fig. 3E–H). Meanwhile, inhibition of NEK7

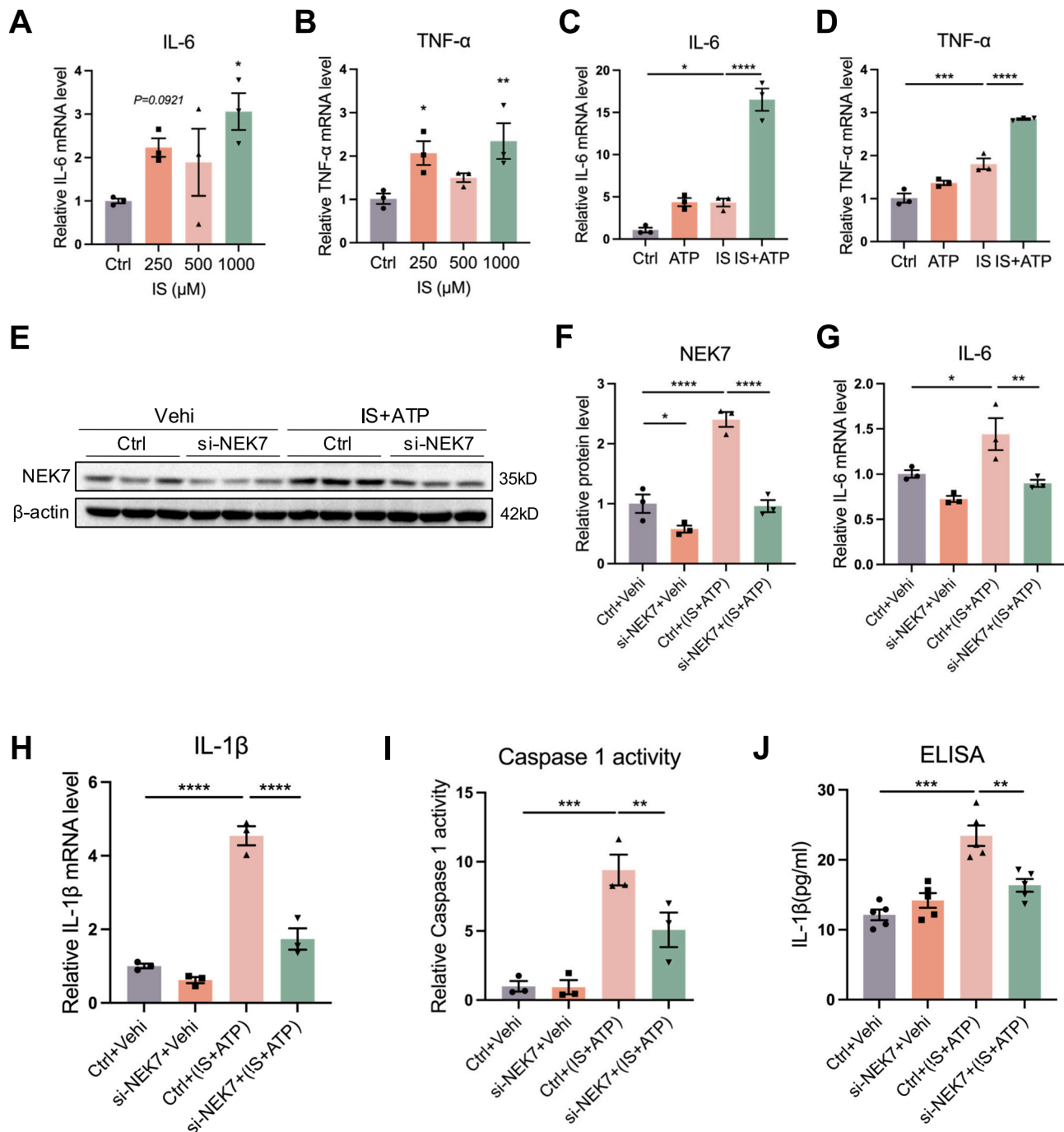


Fig. 3. NEK7 silencing attenuates inflammation in MAECs induced by IS and ATP.

(A–B) Transcript levels of IL-6 and TNF- α in MAECs supplemented with IS for 24 h, $n = 3$. (C–D) IL-6 and TNF- α mRNA levels in MAECs exposed to 1000 μ M IS with or without 5 mM ATP for 24 h, $n = 3$. (E–F) NEK7 protein levels in MAECs transfected with Ctrl (control) or si-NEK7 (NEK7 siRNA), $n = 3$. (G–H) IL-6 and IL-1 β mRNA levels in MAECs within corresponding groups, $n = 3$. Experimental design: after 24-h transfection with Ctrl or NEK7 siRNA, cells were administered IS+ATP or vehicle for an additional 24 h. Caspase 1 activity (I) and IL-1 β release (J) in MAECs in the abovementioned groups, $n = 3$, $n = 5$, respectively. One-way ANOVA followed by Benjamini's multiple comparisons test were used to determine the p-values. * $P < 0.05$, ** $P < 0.01$, *** $P < 0.001$, **** $P < 0.0001$.

significantly weakened the activation of the NLRP3 inflammasome, as shown by the reduced caspase 1 activity (Fig. 3I) and decreased release of IL-1 β (Fig. 3J). To summarize, these data provided solid evidence that NEK7 silencing could impede the activation of the NLRP3 inflammasome and reduce the entire inflammatory level in MAECs induced by IS and ATP.

3.4. Suppression of NEK7 ameliorates IS-induced apoptosis in MAECs

A previous study showed that IS induced apoptosis in MAECs [55], which was also confirmed in our work (Fig. 4A, B, C). Additionally, compared with cells treated with IS alone, the cleaved caspase 3 in MAECs cultured in IS with a combination of ATP was further increased (Fig. 4D, E, F). To identify the potential function of NEK7 in IS-mediated cell apoptosis, we delivered NEK7 siRNA to MAECs and added IS and ATP to the cells for 24 h. We uncovered that the cleaved caspase 3 in the IS+ATP group was markedly reduced in cells with NEK7 inhibition, indicating an amelioration of endothelial injury (Fig. 4G, H, I). Additionally, flow cytometry analysis also showed that knockdown of NEK7 notably inhibited cell death induced by IS and ATP in MAECs (Fig. 4J, K). Collectively, these findings demonstrated that NEK7 deficiency inhibited NLRP3 inflammasome activation, thereby attenuating the endothelium apoptosis triggered by IS and ATP.

3.5. Silencing NLRP3/caspase 1 inhibits caspase 1 activation and cell apoptosis in MAECs induced by IS and ATP

To explore how the NLRP3 inflammasome influences cell damage caused by IS, we transfected MAECs with NLRP3 siRNA followed by treatment with IS and ATP. Through western blotting, we verified that the protein level of NLRP3 was successfully knocked down (Fig. 5A–B). Next, a caspase 1 activity assay kit was used to determine the activity of caspase 1. As shown in Fig. 5C, NLRP3 knockdown greatly attenuated the increment of caspase 1 activity under IS and ATP challenge. Moreover, in NLRP3-knockdown cells, the increased cleaved caspase 3 triggered by IS and ATP was decreased (Fig. 5D–F). The elevated cell death was also decreased, as evidenced by flow cytometry analysis (Fig. 5G–H). Overall, these results validated that NLRP3 silencing could blunt caspase 1 activity and resist the pro-apoptotic effect of IS and ATP administration.

Furthermore, the role of the downstream molecule caspase 1 in NLRP3 inflammasome activation and its associated cell damage were examined. As shown in Fig. 5I–K, administration of caspase 1 siRNA effectively blocked the expression and activity of caspase 1, as evidenced by western blotting and caspase 1 activity assays. Additionally, the cell damage triggered by IS and ATP combination treatment was significantly weakened in the case of caspase 1 suppression, as evidenced by the decreased transcript levels of IL-1 β and TNF- α (Fig. 5L–M) and the downregulated percentage of cell death (Fig. 5N–O). Collectively, these results suggested that inhibition of caspase 1 protected MAECs against the inflammation and apoptosis induced by IS and ATP.

3.6. NEK7/NLRP3/caspase 1 is upregulated and activated in the aortas of 5/6Nx mice

Next, we explored whether the NEK7/NLRP3/caspase 1 pathway was activated in aortic endothelium from mice with ESRD. We first searched the GEO datasets for chronic kidney disease with vascular injury, and found that NEK7 in vein is significantly upregulated in patients with end-stage renal disease (Fig. 6A) [56]. Moreover, in a rat model of CKD (uremia) induced by 5/6Nx operation combined with a high-phosphate diet, transcriptomes of aortas examined by RNA-seq demonstrate an increased NEK7 expression in the uremic aortas compared with the controls (Fig. 6B) [57]. In addition, a DNA microarray expression profile of the thoracic aortas of rats with adenine-induced chronic kidney failure (A-CRF) also shows a marked increase

in NEK7 (Fig. 6C) [58]. These results suggested increased NEK7 in the vascular might play potential importance in ESRD-related CVD.

As mice with 5/6Nx (five-sixths nephrectomy) develop to chronic kidney failure with uremia at 10–12 weeks [59], we performed 5/6Nx or sham operations on C57BL/6 J mice and observed that the kidney function of the mice undergone 5/6Nx was significantly decreased at 12 weeks, as indicated by the increased serum creatinine (Cr) and blood urea nitrogen (BUN) levels (Fig. 6D–E). The expression of NEK7, NLRP3, and caspase 1, and the activity of the NLRP3 inflammasome in the aortic endothelia of these mice were then detected. The results revealed that the protein levels of NEK7, NLRP3, and caspase 1 in the aortas of 5/6Nx mice were markedly increased when compared with the sham mice (Fig. 6F–J). Moreover, there were marked increments in the expression and secretion of IL-1 β in the aortic endothelia and sera from 5/6Nx mice compared with the sham mice, as detected by immunohistochemistry and ELISA (Fig. 6K–M). In addition, dual immunofluorescence staining revealed the enforced colocalization of NLRP3 with ASC in 5/6Nx mice aortas (Fig. 6N–O). These data supported that NLRP3 inflammasomes were activated in the aortic endothelia of mice subjected to 5/6Nx, consistent with the *in vitro* results, suggesting that NEK7-mediated NLRP3 inflammasome activation may be the key mechanism involved in uremic toxin-related endothelial injury.

3.7. NEK7 knockdown diminishes NLRP3 inflammasome activation and alleviates endothelial injury in mice subjected to 5/6Nx

To better validate whether knockdown of NEK7 could inhibit endothelium damage *in vivo*, conditional endothelial cell NEK7-knockout heterozygous mice (Het mice) were generated by crossing NEK7^{fl/fl} mice with Tek-Cre mice (Fig. 7A) and subjected to 5/6Nx operation. We firstly confirmed the reduction of NEK7 in the aortas of Het mice via immunohistochemistry and qRT-PCR (Fig. 7B–D). Consistently with what we mentioned above, the expression and activation of the NLRP3 inflammasome were markedly increased in the aortas from 5/6Nx mice when compared with controls, as characterized by significant upregulation of NEK7, NLRP3, and caspase 1 transcript levels (Fig. 7D–F), marked increments in IL-1 β expression and release (Fig. 7G–I), and enhanced colocalization of NLRP3 with ASC (Fig. 7J–K). All these values were decreased in the aortic endothelium of Het mice challenged with 5/6Nx, indicating a reduction of the NLRP3 inflammasome activation.

Next, we determined the levels of other inflammatory cytokines and the expression of apoptosis-related protein and observed that the increased IL-6, TNF- α , and cleaved caspase 3 in the aortas triggered by 5/6Nx were significantly decreased in Het mice (Fig. 7L–O). These results indicated that NEK7 knockdown markedly attenuated the inflammation and apoptosis in the aortic endothelium of 5/6Nx mice.

Taken together, these results demonstrated that knockdown of NEK7 could impede the activation of the NLRP3 inflammasome and the resulting damage to the aortic endothelium induced by 5/6Nx, supporting that NEK7-mediated NLRP3 inflammasome activation may be an essential mechanism of 5/6Nx-triggered endothelial injury.

3.8. NEK7 overexpression promotes NLRP3 inflammasome activation and exacerbates endothelium apoptosis in mice administered with IS

Furthermore, we investigated the effect of NEK7 overexpression on the aortic endothelium challenged with IS alone *in vivo*. First, NEK7 plasmids were delivered into adult (8 weeks old) C57BL/6 J mice via hydrodynamic tail vein injection to increase the levels of NEK7 in the aorta. Twenty-four hours after NEK7 plasmid injection, the mice received IS (150 mg/kg, *i.p.*) daily for a period of 7 days. NEK7 plasmid injection upregulated the protein and transcript levels of NEK7 in the aorta, whereas the transcript levels of NLRP3 and caspase 1 were not affected (Fig. 8A–B, E–G). IS-injected mice exhibited marked upregulation of NEK7, NLRP3, and caspase 1 in the aorta, consistent with that we observed *in vitro* (Fig. 8A–B, E–G). Although the NEK7/NLRP3/caspase

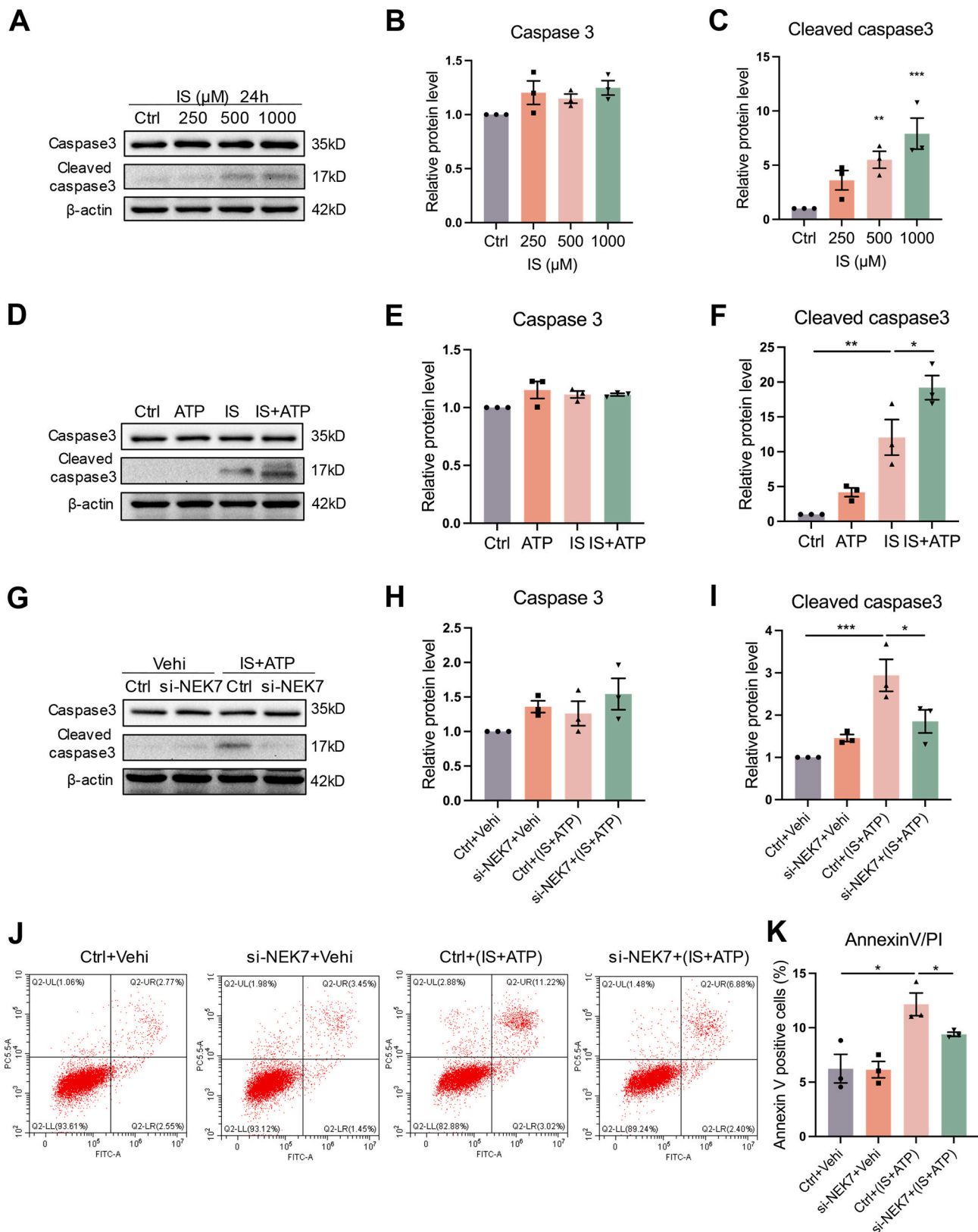


Fig. 4. Suppression of NEK7 ameliorates IS-induced apoptosis in MAECs.

(A–C) Caspase 3 and cleaved caspase 3 protein levels in MAECs exposed to ascend concentrations (250, 500, and 1000 μM) of IS for 24 h, n = 3. (D–F) Protein levels of caspase 3 and cleaved caspase 3 in MAECs exposed to 1000 μM IS with or without 5 mM ATP for 24 h analyzed by western blotting, n = 3. Caspase 3 and cleaved caspase 3 levels in MAECs by western blotting analysis (G–I) and proportion of cell death through flow cytometry analysis following FITC Annexin V labeling (J–K), n = 3. One-way ANOVA followed by Benjamini's multiple comparisons test were used to determine the p-values. **P* < 0.05, ***P* < 0.01, ****P* < 0.001.

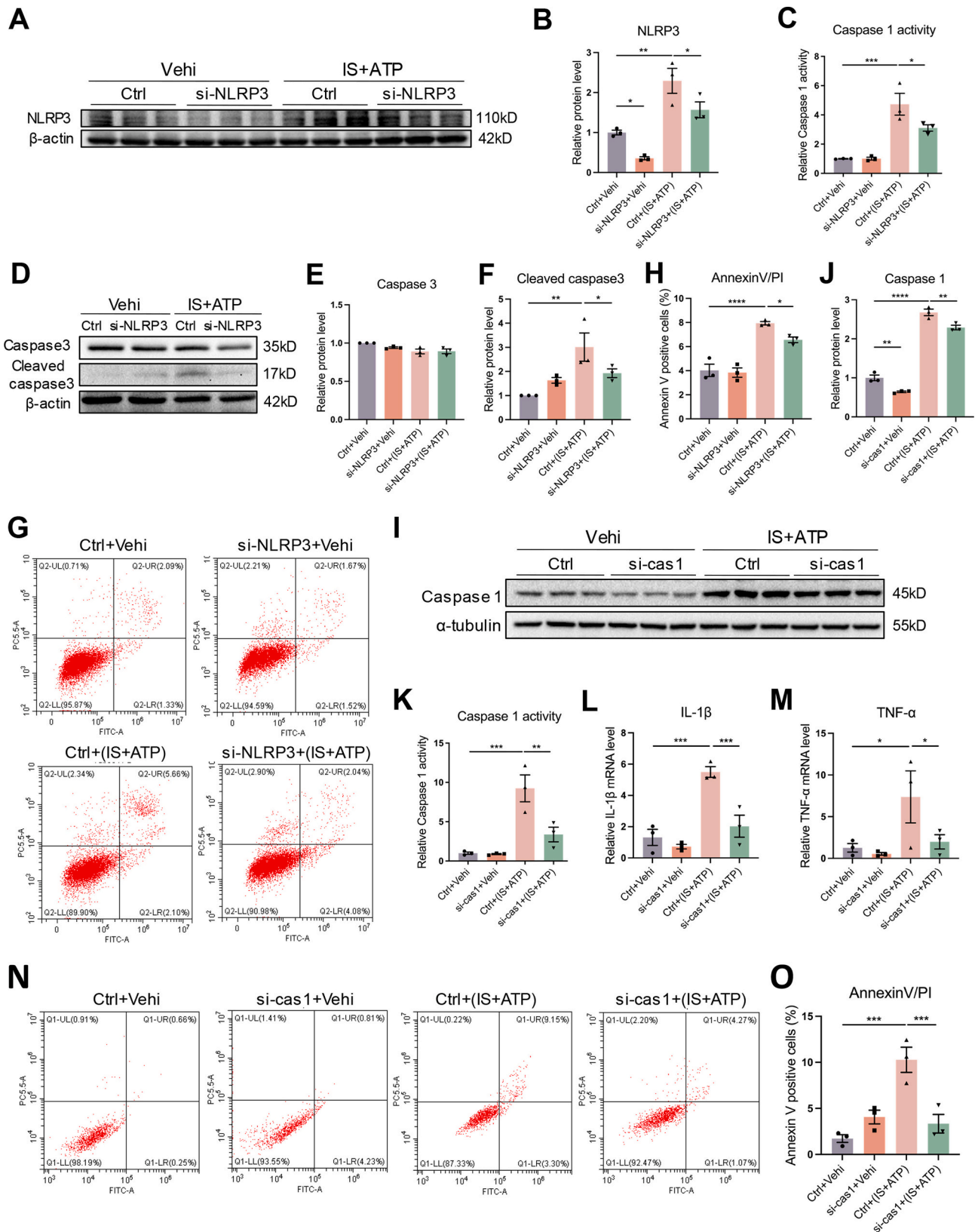


Fig. 5. Silencing NLRP3/caspase 1 inhibits caspase 1 activation and cell apoptosis in MAECs induced by IS and ATP.

(A–B) Efficiency of si-NLRP3 (NLRP3 siRNA) in MAECs examined by western blotting, $n = 3$. Caspase 1 activity (C), caspase 3 and cleaved caspase 3 protein levels (D–F), and cell death (G–H) in MAECs incubated with IS+ATP for 24 h after si-NLRP3 transfection, $n = 3$. (I–J) Silencing efficiency of caspase 1 siRNA, as detected by western blotting, $n = 3$. Caspase 1 activity (K), IL-1 β and TNF- α mRNA levels (L–M) and cell death (N–O) in MAECs within each group following the indicated treatments, $n = 3$. Experimental design: after 24-h transfection with Ctrl or caspase 1 siRNA, cells were administered IS+ATP or vehicle for an additional 24 h. One-way ANOVA followed by Benjamini's multiple comparisons test were used to determine the p -values. * $P < 0.05$, ** $P < 0.01$, *** $P < 0.001$, **** $P < 0.0001$.

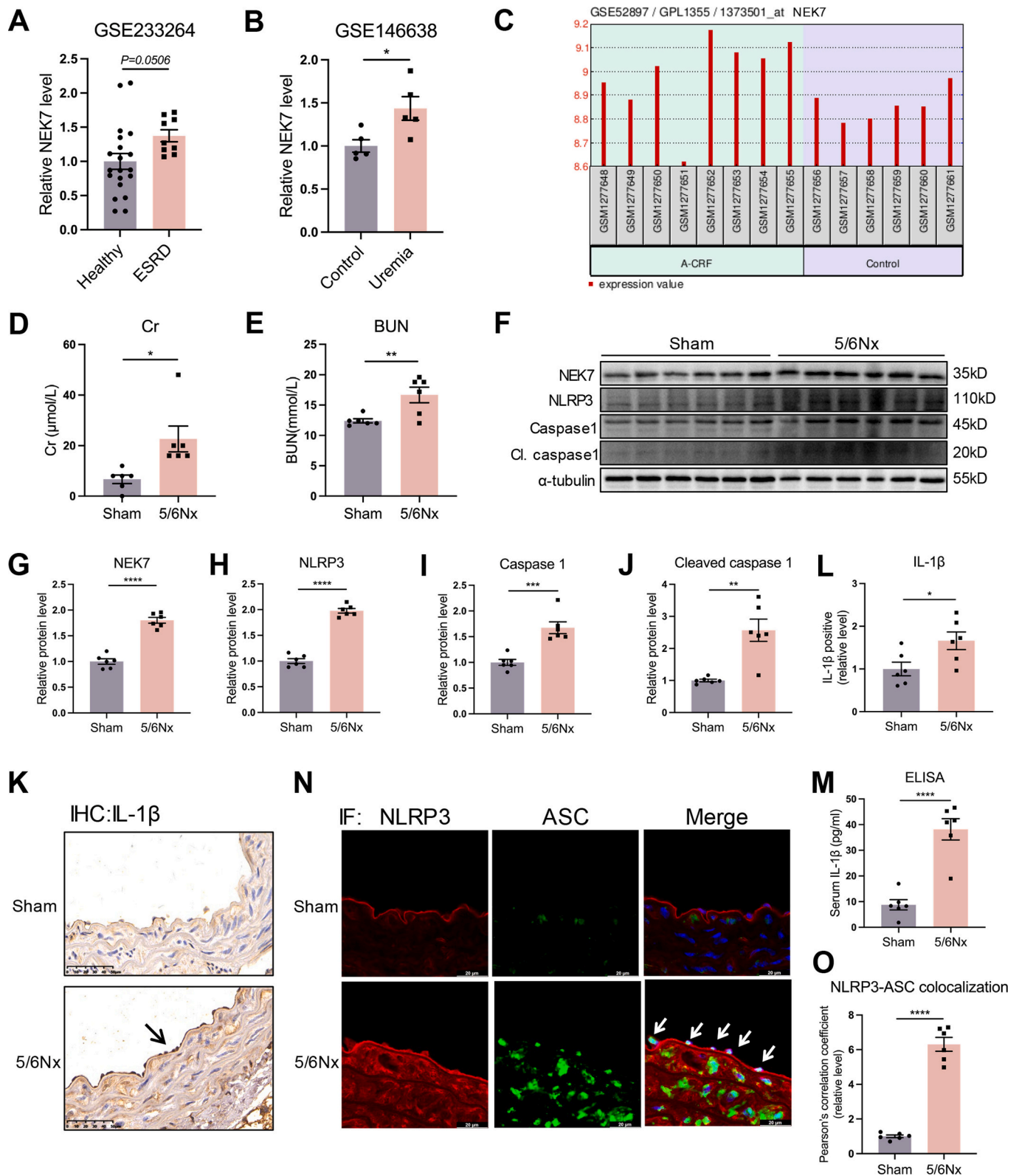
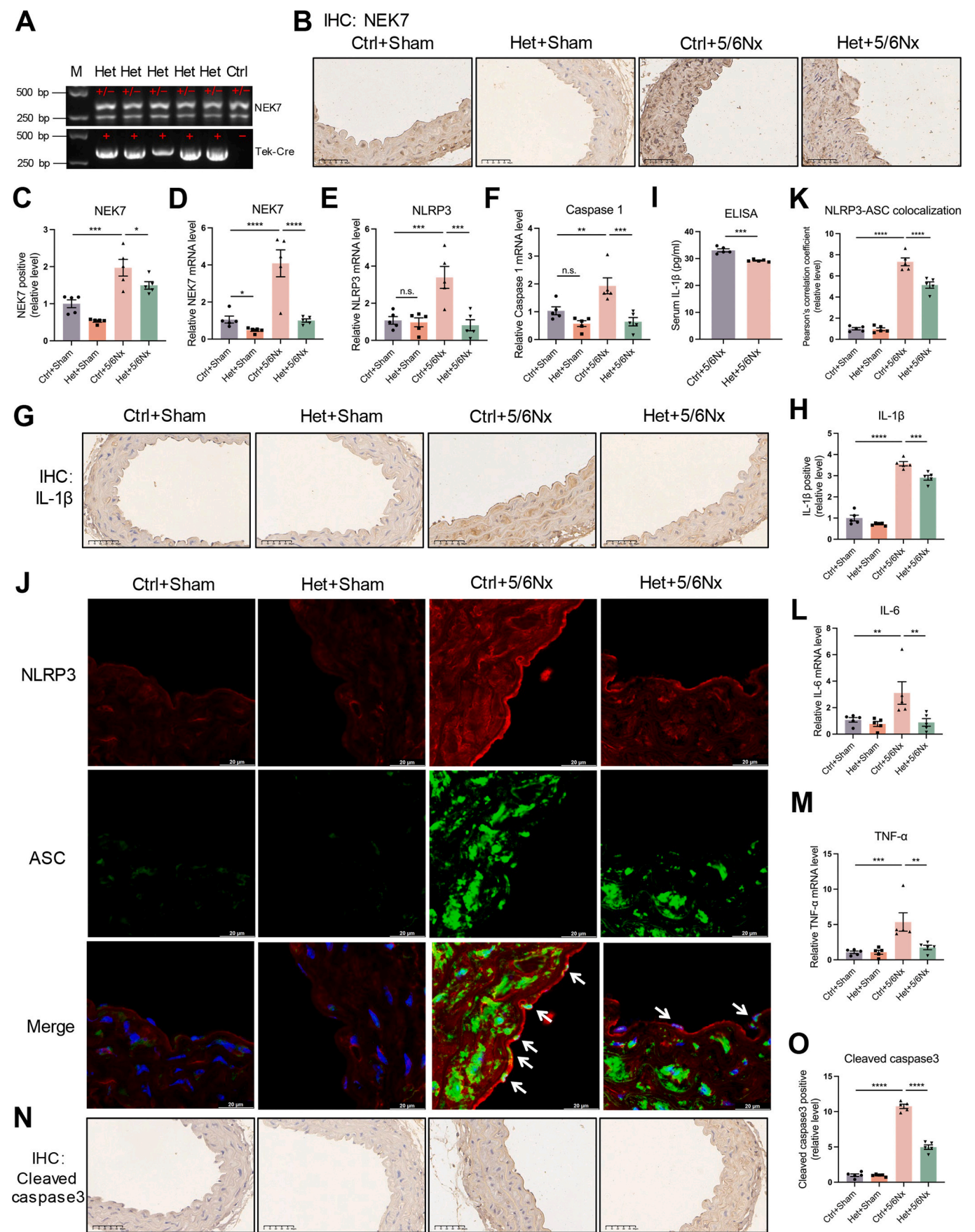


Fig. 6. NEK7/NLRP3/caspase 1 is upregulated and activated in the aortas of 5/6Nx mice. (A–C) Relative NEK7 gene levels in several reported uremia-related models by analyzing the corresponding gene expression profiles of GEO datasets from PubMed (GSE233264, GSE146638, GSE52897). (D–E) Levels of Cr and BUN in sera from the 5/6Nx mice and control mice (sham), $n = 6$. (F–J) Western blot analysis of NEK7, NLRP3, and caspase 1 expression in the aortic tissues of 5/6Nx and sham mice, $n = 6$. (K–L) IL-1 β levels in the aortas of 5/6Nx and sham mice, shown by representative IHC images, scale bars: 20 μm , $n = 6$. Activation of the NLRP3 inflammasome in 5/6Nx and control mice, shown respectively by serum IL-1 β levels (M) and NLRP3-ASC colocalization (N–O), $n = 6$. Two-tailed unpaired t -test were used to determine the p -values. $*P < 0.05$, $**P < 0.01$, $***P < 0.001$, $****P < 0.0001$.



(caption on next page)

Fig. 7. NEK7 knockdown diminishes NLRP3 inflammasome activation and alleviates endothelial injury in mice subjected to 5/6Nx.

(A) Genotyping of NEK7 knockout mice by PCR analysis. Het mice, endothelial cell-specific NEK7 knockout heterozygotes; +/−, heterozygous NEK7^{fl/fl} mice; +, Tek-Cre (+) mice; −, Tek-Cre (−) mice; M, DNA marker. (B–C) Expression of NEK7 in Het mice and their littermates (Ctrl mice), shown by representative IHC images, scale bars: 20 μm, n = 5. (D–F) Transcript levels of NEK7, NLRP3, and caspase 1 in the aortic endothelium from the 5/6Nx and sham groups of Het and Ctrl mice, n = 5. (G–I) IL-1β expression in the aortas determined by immunohistochemistry and IL-1β release in the serum examined by ELISA, n = 5. (J–K) Representative dual immunofluorescence images of NLRP3-ASC colocalization in the aortic endothelium from above-mentioned four groups of mice, scale bars: 20 μm, n = 5. (L–O) Endothelial inflammation and apoptosis in the 5/6Nx and sham groups of Het and Ctrl mice, determined by transcript levels of IL-6 and TNF-α (n = 5) and protein level of cleaved caspase3 (n = 5). Two-tailed unpaired t-test were used to determine the p-values for I. One-way ANOVA followed by Benjamini's multiple comparisons test were used to determine the p-values for the others. *P < 0.05, **P < 0.01, ***P < 0.001, ****P < 0.0001.

1 upregulated by IS did not further increase under NEK7 overexpression, the levels of both IL-1β release and NLRP3-ASC colocalization were enhanced (Fig. 8H–J). Additionally, the IS-induced expression of cleaved caspase 3 in the mouse aortic endothelium was further increased upon NEK7 upregulation, as shown by western blotting (Fig. 8A, C–D). These findings indicated that the NLRP3 inflammasome in the aortas of mice with IS overdose was primed, which could be further activated by NEK7 upregulation, suggesting that NEK7-mediated NLRP3 inflammasome activation may be an important mechanism of IS-induced damage to the aortic endothelium.

4. Discussion

Cardiovascular disease (CVD) in ESRD is closely associated with the toxicity of accumulated uremic wastes (e.g., IS, the most extensively studied) to vascular endothelial cells [60–62]. A previous work uncovered how the NLRP3 inflammasome triggers endothelial inflammation [63]. Additionally, NEK7 has been shown to mediate the activation of the NLRP3 inflammasome [40,41]. However, few studies have been conducted to examine the participation of NEK7-mediated NLRP3 inflammasome activation in IS-related endothelial injury, highlighting an urgent need for further investigation.

In the current research, we elucidated the effect of the NEK7-activated NLRP3 inflammasome in IS-induced endothelial injury. Here, we observed that IS only upregulated the levels of NEK7, NLRP3, and caspase 1, but did not induced the activation of NLRP3 inflammasome in MAECs, suggesting that IS might play an essential part in the priming of the NLRP3 inflammasome, which is a prerequisite for its subsequent activation. To induce NLRP3 inflammasome activation, an additional trigger, such as ATP, pore-forming toxins, or crystals, is necessary [53]. In the uremia stage of ESRD, accumulated toxins in the body induced various DAMPs (ATP, ROS, et al.) release [64–66]. Therefore, in the following in-vitro experiments, we used one of the DAMPs—ATP to treated MAECs together with IS. Although ATP did not increase the IS-induced upregulation of NEK7, NLRP3, and caspase 1, the NLRP3 inflammasome was further activated by the combination treatment of IS with ATP. These results suggest the determining function of the activated NLRP3 inflammasome in IS-related endothelial damage.

We subsequently reduced the levels of NEK7, NLRP3, and caspase 1 in MAECs using corresponding siRNAs. We found that depletion of NEK7, NLRP3, or caspase 1 reduced NLRP3 inflammasome activation and alleviated the inflammation and apoptosis induced by treatment with IS and ATP. These results confirmed the important mechanism of NEK7-mediated NLRP3 inflammasome activation in IS-related endothelial damage. Therefore, we speculated that IS-upregulated NEK7 might contribute to endothelial injury by amplifying NLRP3 inflammasome activation.

The 5/6Nx is the most classical model to trigger ESRD-related uremia [59]. We performed 5/6Nx operations and found that both NEK7 expression and activation of the NLRP3 inflammasome were greatly increased. In line with the in vitro results, endothelial cell-specific NEK7 knockdown mice exhibited restored activation of the NLRP3 inflammasome and improved endothelial injury when challenged with 5/6Nx. These results verified the potential role of NEK7 in mediating ESRD-related endothelial damage through NLRP3 inflammasome activation. Additionally, IS alone administration in vivo not only upregulated the

expression of the NLRP3 inflammasome components, but also induced the activation of NLRP3 inflammasome, as evidenced by increased active caspase 1, serum IL-1β, and increased overlap of ASC and NLRP3 in the aorta compared with the control mice. This may be due to IS-induced systemic cascade damage and inflammation (including vascular endothelial cells, immune cells, etc.) that resulted in the release of various DAMPs (ATP, ROS, et al.) in vivo [64–66], which then synergistically acts as the second hit to activate the NLRP3 inflammasome. However, in vitro, IS acts on only one layer of endothelial cells, releasing a relatively lower level of DAMPs due to the loss of amplification loops between different types of cells, and the amount of released DAMPs from endothelial cells in plate may be not sufficient to synergistically trigger NLRP3 inflammasome activation. Thus, ATP was additionally provided in vitro but not in vivo in this study. Additionally, activation of the NLRP3 inflammasome was pronounced upon NEK7 overexpression, exacerbating aortic endothelium apoptosis induced by IS in the mice. These results further confirmed the fundamental role of NEK7 in NLRP3 inflammasome activation and endothelium injury induced by IS.

Our work only focused on the role of a single uremic toxin in endothelial damage. Because substantial uremic toxins accumulate in cases of end-stage renal disease, further investigations should be conducted to reveal their potential synergic effects on endothelial cells through the simultaneous use of multiple uremic toxins. Additionally, it would be better to confirm the critical role of NEK7 through endothelial activation and suppression of NLRP3 in vivo, which is the limitation of this study.

In conclusion, we investigated and elucidated the key regulation of NEK7-activated NLRP3 inflammasome in IS-induced endothelial injury. The results not only revealed a mechanism of IS-mediated endothelial injury in ESRD, but also provide a putative therapeutic target for ESRD-related CVD. Further investigations involving pharmacological interventions of NEK7 (e.g., develop NEK7 inhibitors) to validate the therapeutic potential in ameliorating vascular injury and mortality in ESRD, would bring greater clinical significance.

CRedit authorship contribution statement

Le Sun: Writing – review & editing, Writing – original draft, Visualization, Software, Investigation, Formal analysis. **Ying Ren:** Writing – review & editing, Methodology, Investigation, Formal analysis. **Wenping Zhu:** Writing – review & editing, Validation, Methodology, Investigation. **Tong Ni:** Methodology, Investigation. **Songming Huang:** Writing – review & editing, Validation. **Aihua Zhang:** Writing – review & editing, Conceptualization. **Yue Zhang:** Writing – review & editing, Methodology. **Hu Hua:** Supervision, Methodology, Formal analysis, Data curation. **Zhanjun Jia:** Writing – review & editing, Supervision, Resources, Conceptualization. **Zhenzhen Sun:** Writing – review & editing, Supervision, Methodology, Funding acquisition, Data curation, Conceptualization.

Funding sources

This work was supported by funding from the National Natural Science Foundation of China (81700651) and Postgraduate Research & Practice Innovation Program of Jiangsu Province (KYCX25_2154, JX12214136).

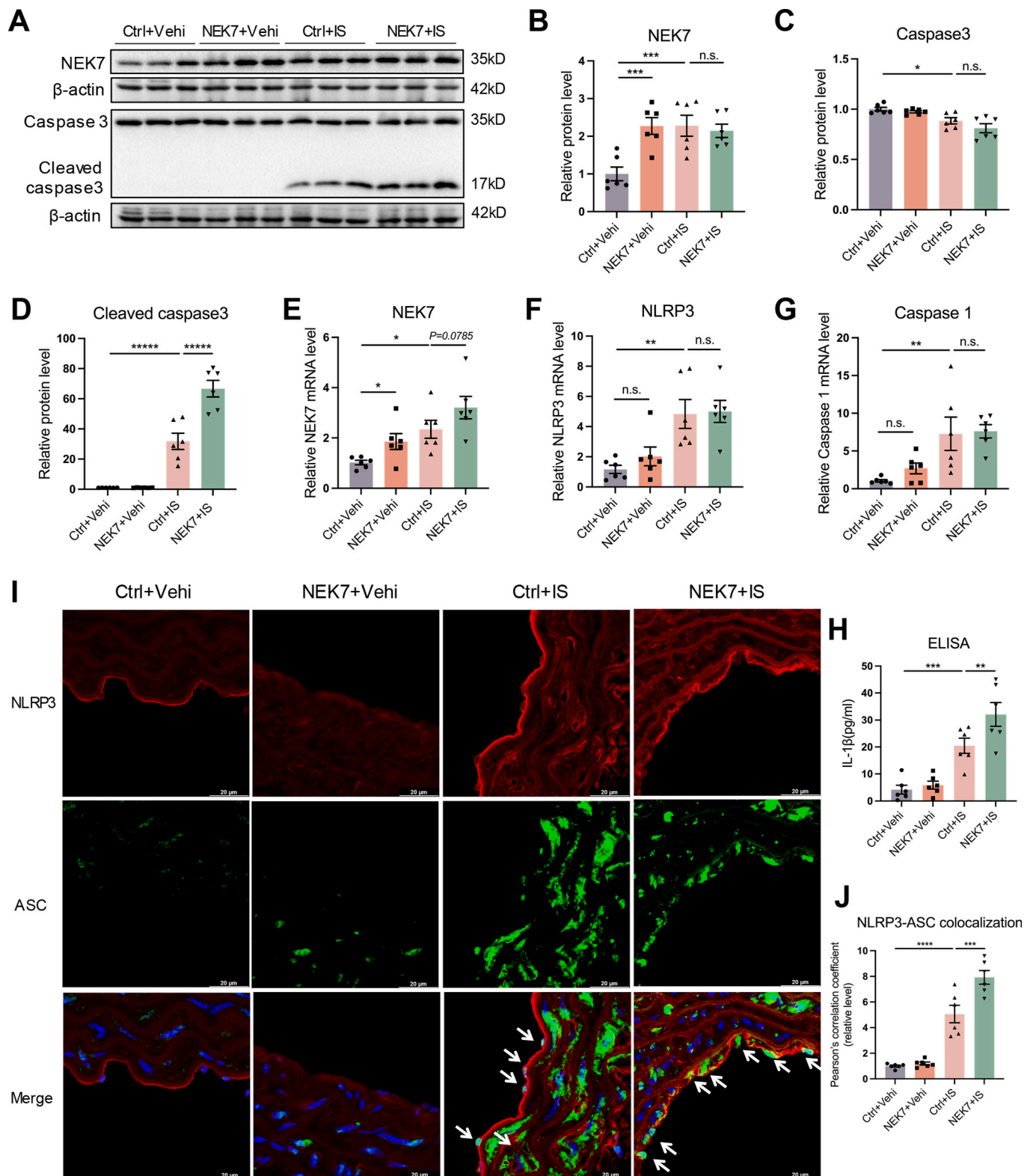


Fig. 8. NEK7 overexpression promotes NLRP3 inflammasome activation and exacerbates endothelium apoptosis in mice administered with IS. (A–D) NEK7, caspase 3 and cleaved caspase 3 protein levels in the aortic tissues of mice after hydrodynamic tail vein injection of NEK7 and Ctrl plasmids followed by IS administration for 7 consecutive days, $n = 6$. (E–G) NEK7, NLRP3, and caspase 1 mRNA levels in aortas from the four groups of mice, $n = 6$. The contribution of NEK7 to IS-induced NLRP3 inflammasome activation in vivo, demonstrated by the release of IL-1 β by ELISA (H) and the colocalization of NLRP3 with ASC by dual immunofluorescence staining (I–J), $n = 6$. One-way ANOVA followed by Benjamini's multiple comparisons test were used to determine the p-values. * $P < 0.05$, ** $P < 0.01$, *** $P < 0.001$, **** $P < 0.0001$.

Declaration of competing interest

The authors declare that they have no known competing financial interests or personal relationships that could have appeared to influence the work reported in this paper.

Acknowledgements

We appreciate LetPub (www.letpub.com.cn) for providing linguistic support throughout the manuscript preparation.

Appendix A. Supplementary data

Supplementary data to this article can be found online at <https://doi.org/10.1016/j.intimp.2025.115236>.

Data availability

Data and used sequences information are provided within the manuscript or supplementary information files. The original data is available from the corresponding author upon reasonable request.

References

- [1] (2024) KDIGO, Clinical practice guideline for the evaluation and Management of Chronic Kidney Disease, *Kidney Int.* 105 (2024) S117–S314, <https://doi.org/10.1016/j.kint.2023.10.018>.
- [2] P. August, Chronic kidney disease - another step forward, *N. Engl. J. Med.* 388 (2023) 179–180, <https://doi.org/10.1056/NEJMe2215286>.
- [3] Y.N. Wang, S.X. Ma, Y.Y. Chen, L. Chen, B.L. Liu, Q.Q. Liu, et al., Chronic kidney disease: biomarker diagnosis to therapeutic targets, *Clin. Chim. Acta* 499 (2019) 54–63, <https://doi.org/10.1016/j.cca.2019.08.030>.
- [4] K. Wang, Q. Liu, M. Tang, G. Qi, C. Qiu, Y. Huang, et al., Chronic kidney disease-induced muscle atrophy: molecular mechanisms and promising therapies, *Biochem. Pharmacol.* 208 (2023) 115407, <https://doi.org/10.1016/j.bcp.2022.115407>.
- [5] Y. Liu, Kidney fibrosis: fundamental questions, challenges, and perspectives, *Integrative Med. Nephrology Androl.* 11 (2024) e24–00027, <https://doi.org/10.1097/imna-d-24-00027>.
- [6] X. Li, B. Lindholm, Cardiovascular risk prediction in chronic kidney disease, *Am. J. Nephrol.* 53 (2022) 730–739, <https://doi.org/10.1159/000528560>.
- [7] K. Vijay, B.L. Neuen, E.V. Lerma, Heart failure in patients with diabetes and chronic kidney disease: challenges and opportunities, *Cardiorenal Med.* 12 (2022) 1–10, <https://doi.org/10.1159/000520909>.
- [8] S.A. Hebert, H.N. Ibrahim, Hypertension Management in Patients with chronic kidney disease, *Methodist Debaque Cardiovasc. J.* 18 (2022) 41–49, <https://doi.org/10.14797/mdcvj.1119>.
- [9] N. Marx, J. Floege, Cardiovascular disease in patients with chronic kidney disease, *Herz* 46 (2021) 205, <https://doi.org/10.1007/s00059-021-05029-y>.
- [10] Y. Mok, S.H. Ballew, K. Matsushita, Chronic kidney disease measures for cardiovascular risk prediction, *Atherosclerosis* 335 (2021) 110–118, <https://doi.org/10.1016/j.atherosclerosis.2021.09.007>.
- [11] E. Ku, B.J. Lee, J. Wei, M.R. Weir, Hypertension in CKD: Core curriculum 2019, *Am. J. Kidney Dis.* 74 (2019) 120–131, <https://doi.org/10.1053/j.ajkd.2018.12.044>.
- [12] M.H. Rosner, T. Reis, F. Husain-Syed, R. Vanholder, C. Hutchison, P. Stenvinkel, et al., Classification of uremic toxins and their role in kidney failure, *Clin. J. Am. Soc. Nephrol.* 16 (2021) 1918–1928, <https://doi.org/10.2215/cjn.02660221>.
- [13] F. Duranton, G. Cohen, R. De Smet, M. Rodriguez, J. Jankowski, R. Vanholder, et al., Normal and pathologic concentrations of uremic toxins, *J. Am. Soc. Nephrol.* 23 (2012) 1258–1270, <https://doi.org/10.1681/asn.2011121175>.
- [14] S.C. Leong, T.L. Sirich, Indoxyl sulfate-review of toxicity and therapeutic strategies, *Toxins (Basel)*. 8 (2016), <https://doi.org/10.3390/toxins8120358>.
- [15] T.H. Cheng, M.C. Ma, M.T. Liao, C.M. Zheng, K.C. Lu, C.H. Liao, et al., Indoxyl sulfate, a tubular toxin, contributes to the development of chronic kidney disease, *Toxins (Basel)*. 12 (2020), <https://doi.org/10.3390/toxins12110684>.
- [16] W.C. Liu, Y. Tomino, K.C. Lu, Impacts of Indoxyl sulfate and p-cresol sulfate on chronic kidney disease and mitigating effects of AST-120, *Toxins (Basel)*. 10 (2018), <https://doi.org/10.3390/toxins10090367>.
- [17] G. Lano, S. Burtay, M. Sallée, Indoxyl sulfate, a uremic Endotheliotoxin, *Toxins (Basel)*. 12 (2020), <https://doi.org/10.3390/toxins12040229>.
- [18] J. Pei, R. Juni, M. Harakalova, D.J. Duncker, F.W. Asselbergs, P. Koolwijk, et al., Indoxyl sulfate stimulates angiogenesis by regulating reactive oxygen species production via CYP1B1, *Toxins (Basel)*. 11 (2019), <https://doi.org/10.3390/toxins11080454>.
- [19] J.H. Ryu, H. Park, S.J. Kim, The effects of indoxyl sulfate-induced endothelial microparticles on neointimal hyperplasia formation in an ex vivo model, *Ann Surg Treat Res.* 93 (2017) 11–17, <https://doi.org/10.4174/astr.2017.93.1.11>.
- [20] A. García-Jérez, A. Luengo, J. Carracedo, R. Ramírez-Chamond, D. Rodríguez-Puyol, M. Rodríguez-Puyol, et al., Effect of uraemia on endothelial cell damage is mediated by the integrin linked kinase pathway, *J. Physiol.* 593 (2015) 601–618, discussion 18, <https://doi.org/10.1113/jphysiol.2014.283887>.
- [21] P.C. Fan, J.C. Chang, C.N. Lin, C.C. Lee, Y.T. Chen, P.H. Chu, et al., Serum indoxyl sulfate predicts adverse cardiovascular events in patients with chronic kidney disease, *J. Formos. Med. Assoc.* 118 (2019) 1099–1106, <https://doi.org/10.1016/j.jfma.2019.03.005>.
- [22] W.C. Shen, C.J. Liang, T.M. Huang, C.W. Liu, S.H. Wang, G.H. Young, et al., Indoxyl sulfate enhances IL-1 β -induced E-selectin expression in endothelial cells in acute kidney injury by the ROS/MAPKs/NF κ B/AP-1 pathway, *Arch. Toxicol.* 90 (2016) 2779–2792, <https://doi.org/10.1007/s00204-015-1652-0>.
- [23] S. Ito, Y. Higuchi, Y. Yagi, F. Nishijima, H. Yamato, H. Ishii, et al., Reduction of indoxyl sulfate by AST-120 attenuates monocyte inflammation related to chronic kidney disease, *J. Leukoc. Biol.* 93 (2013) 837–845, <https://doi.org/10.1189/jlb.0112023>.
- [24] K. Nakagawa, M. Itoya, N. Takemoto, Y. Matsuura, M. Tawa, Y. Matsumura, et al., Indoxyl sulfate induces ROS production via the aryl hydrocarbon receptor-NADPH oxidase pathway and inactivates NO in vascular tissues, *Life Sci.* 265 (2021) 118807, <https://doi.org/10.1016/j.lfs.2020.118807>.
- [25] V.C. Wu, G.H. Young, P.H. Huang, S.C. Lo, K.C. Wang, C.Y. Sun, et al., In acute kidney injury, indoxyl sulfate impairs human endothelial progenitor cells: modulation by statin, *Angiogenesis* 16 (2013) 609–624, <https://doi.org/10.1007/s10456-013-9339-8>.
- [26] Y. Luo, Z. Tan, Y. Ye, X. Ma, G. Yue, Qiqlan ameliorates vascular endothelial dysfunction by inhibiting NLRP3-ASC inflammasome activation in vivo and in vitro, *Pharm. Biol.* 61 (2023) 815–824, <https://doi.org/10.1080/13880209.2023.2208617>.
- [27] Y. Liu, H.L. Yin, C. Li, F. Jiang, S.J. Zhang, X.R. Zhang, et al., Sinapine thiocyanate ameliorates vascular endothelial dysfunction in hypertension by inhibiting activation of the NLRP3 Inflammasome, *Front. Pharmacol.* 11 (2020) 620159, <https://doi.org/10.3389/fphar.2020.620159>.
- [28] L. Dai, L. Zhu, S. Ma, J. Liu, M. Zhang, J. Li, et al., Berberine alleviates NLRP3 inflammasome induced endothelial junction dysfunction through ca(2+) signalling in inflammatory vascular injury, *Phytomedicine* 101 (2022) 154131, <https://doi.org/10.1016/j.phymed.2022.154131>.
- [29] X. Li, Z. Zhang, M. Luo, Z. Cheng, R. Wang, Q. Liu, et al., NLRP3 inflammasome contributes to endothelial dysfunction in angiotensin II-induced hypertension in mice, *Microvasc. Res.* 143 (2022) 104384, <https://doi.org/10.1016/j.mvr.2022.104384>.
- [30] D. Zheng, Z. Shi, M. Yang, B. Liang, X. Zhou, L. Jing, et al., NLRP3 inflammasome-mediated endothelial cells pyroptosis is involved in decabromodiphenyl ethane-induced vascular endothelial injury, *Chemosphere* 267 (2021) 128867, <https://doi.org/10.1016/j.chemosphere.2020.128867>.
- [31] K. Liao, D.Y. Lv, H.L. Yu, H. Chen, S.X. Luo, iNOS regulates activation of the NLRP3 inflammasome through the sGC/cGMP/PKG/TACE/TNF- α axis in response to cigarette smoke resulting in aortic endothelial pyroptosis and vascular dysfunction, *Int. Immunopharmacol.* 101 (2021) 108334, <https://doi.org/10.1016/j.intimp.2021.108334>.
- [32] H. Ito, H. Kimura, T. Karasawa, S. Hisata, A. Sadatomo, Y. Inoue, et al., NLRP3 Inflammasome activation in lung vascular endothelial cells contributes to intestinal ischemia/reperfusion-induced acute lung injury, *J. Immunol.* 205 (2020) 1393–1405, <https://doi.org/10.4049/jimmunol.2000217>.
- [33] X. Zhou, Y. Wu, L. Ye, Y. Wang, K. Zhang, L. Wang, et al., Aspirin alleviates endothelial gap junction dysfunction through inhibition of NLRP3 inflammasome activation in LPS-induced vascular injury, *Acta Pharm. Sin. B* 9 (2019) 711–723, <https://doi.org/10.1016/j.apsb.2019.02.008>.
- [34] K.M. Boini, T. Hussain, P.L. Li, S. Koka, Trimethylamine-N-oxide instigates NLRP3 Inflammasome activation and endothelial dysfunction, *Cell. Physiol. Biochem.* 44 (2017) 152–162, <https://doi.org/10.1159/000484623>.
- [35] X. Sun, X. Jiao, Y. Ma, Y. Liu, L. Zhang, Y. He, et al., Trimethylamine N-oxide induces inflammation and endothelial dysfunction in human umbilical vein endothelial cells via activating ROS-TXNIP-NLRP3 inflammasome, *Biochem. Biophys. Res. Commun.* 481 (2016) 63–70, <https://doi.org/10.1016/j.bbrc.2016.11.017>.
- [36] J. Fu, H. Wu, Structural mechanisms of NLRP3 Inflammasome assembly and activation, *Annu. Rev. Immunol.* 41 (2023) 301–316, <https://doi.org/10.1146/annurev-immunol-081022-021207>.
- [37] J. Wang, S. Chen, M. Liu, M. Zhang, X. Jia, NEK7: a new target for the treatment of multiple tumors and chronic inflammatory diseases, *Inflammopharmacology* 30 (2022) 1179–1187, <https://doi.org/10.1007/s10787-022-01026-7>.
- [38] E.E. de Souza, G.V. Meirelles, B.B. Godoy, A.M. Perez, J.H. Smetana, S.J. Doxsey, et al., Characterization of the human NEK7 interactome suggests catalytic and regulatory properties distinct from those of NEK6, *J. Proteome Res.* 13 (2014) 4074–4090, <https://doi.org/10.1021/pr500437x>.
- [39] S. Zheng, X. Que, S. Wang, Q. Zhou, X. Xing, L. Chen, et al., ZDHHC5-mediated NLRP3 palmitoylation promotes NLRP3-NEK7 interaction and inflammasome activation, *Mol. Cell* 83 (2023), <https://doi.org/10.1016/j.molcel.2023.11.015>, 4570–85.e7.
- [40] H. Sharif, L. Wang, W.L. Wang, V.G. Magupalli, L. Andreeva, Q. Qiao, et al., Structural mechanism for NEK7-licensed activation of NLRP3 inflammasome, *Nature* 570 (2019) 338–343, <https://doi.org/10.1038/s41586-019-1295-z>.
- [41] Y. He, M.Y. Zeng, D. Yang, B. Motro, G. Núñez, NEK7 is an essential mediator of NLRP3 activation downstream of potassium efflux, *Nature* 530 (2016) 354–357, <https://doi.org/10.1038/nature16959>.

- [42] H. Shi, Y. Wang, X. Li, X. Zhan, M. Tang, M. Fina, et al., NLRP3 activation and mitosis are mutually exclusive events coordinated by NEK7, a new inflammasome component, *Nat. Immunol.* 17 (2016) 250–258, <https://doi.org/10.1038/ni.3333>.
- [43] W. Gong, S. Mao, J. Yu, J. Song, Z. Jia, S. Huang, et al., NLRP3 deletion protects against renal fibrosis and attenuates mitochondrial abnormality in mouse with 5/6 nephrectomy, *Am. J. Physiol. Ren. Physiol.* 310 (2016) F1081–F1088, <https://doi.org/10.1152/ajprenal.00534.2015>.
- [44] G. Lin, N. Li, D. Li, L. Chen, H. Deng, S. Wang, et al., Carnosic acid inhibits NLRP3 inflammasome activation by targeting both priming and assembly steps, *Int. Immunopharmacol.* 116 (2023) 109819, <https://doi.org/10.1016/j.intimp.2023.109819>.
- [45] Y. Zhang, L. Luo, X. Xu, J. Wu, F. Wang, Y. Lu, et al., Acetylation is required for full activation of the NLRP3 inflammasome, *Nat. Commun.* 14 (2023) 8396, <https://doi.org/10.1038/s41467-023-44203-0>.
- [46] C. Hamilton, A. Olona, S. Leishman, K. MacDonald-Ramsahai, S. Cockcroft, G. Larrouy-Maumus, et al., NLRP3 Inflammasome priming and activation are regulated by a phosphatidylinositol-dependent mechanism, *Immunohorizons* 6 (2022) 642–659, <https://doi.org/10.4049/imunohorizons.2200058>.
- [47] D.W. Shim, H.J. Cho, I. Hwang, T.Y. Jung, H.S. Kim, J.H. Ryu, et al., Intracellular NAD(+) depletion confers a priming signal for NLRP3 Inflammasome activation, *Front. Immunol.* 12 (2021) 765477, <https://doi.org/10.3389/fimmu.2021.765477>.
- [48] X. Lin, H. Wang, X. An, J. Zhang, J. Kuang, J. Hou, et al., Baecklein E suppressed NLRP3 inflammasome activation through inhibiting both the priming and assembly procedure: implications for gout therapy, *Phytomedicine* 84 (2021) 153521, <https://doi.org/10.1016/j.phymed.2021.153521>.
- [49] Y. Xu, Q. Yuan, S. Cao, S. Cui, L. Xue, X. Song, et al., Aldehyde dehydrogenase 2 inhibited oxidized LDL-induced NLRP3 inflammasome priming and activation via attenuating oxidative stress, *Biochem. Biophys. Res. Commun.* 529 (2020) 998–1004, <https://doi.org/10.1016/j.bbrc.2020.06.075>.
- [50] Y. Long, X. Liu, X.Z. Tan, C.X. Jiang, S.W. Chen, G.N. Liang, et al., ROS-induced NLRP3 inflammasome priming and activation mediate PCB 118- induced pyroptosis in endothelial cells, *Ecotoxicol. Environ. Saf.* 189 (2020) 109937, <https://doi.org/10.1016/j.ecoenv.2019.109937>.
- [51] A. Gritsenko, S. Yu, F. Martin-Sanchez, I. Diaz-Del-Olmo, E.M. Nichols, D.M. Davis, et al., Priming is dispensable for NLRP3 Inflammasome activation in human monocytes in vitro, *Front. Immunol.* 11 (2020) 565924, <https://doi.org/10.3389/fimmu.2020.565924>.
- [52] S. Son, D.W. Shim, I. Hwang, J.H. Park, J.W. Yu, Chemotherapeutic agent paclitaxel mediates priming of NLRP3 Inflammasome activation, *Front. Immunol.* 10 (2019) 1108, <https://doi.org/10.3389/fimmu.2019.01108>.
- [53] S. Paik, J.K. Kim, P. Silwal, C. Sasakawa, E.K. Jo, An update on the regulatory mechanisms of NLRP3 inflammasome activation, *Cell. Mol. Immunol.* 18 (2021) 1141–1160, <https://doi.org/10.1038/s41423-021-00670-3>.
- [54] H. Cui, S. Banerjee, N. Xie, T. Dey, R.M. Liu, Y.Y. Sanders, et al., MafB regulates NLRP3 inflammasome activation by sustaining p62 expression in macrophages, *Commun Biol.* 6 (2023) 1047, <https://doi.org/10.1038/s42003-023-05426-5>.
- [55] S. Li, Y. Xie, B. Yang, S. Huang, Y. Zhang, Z. Jia, et al., MicroRNA-214 targets COX-2 to antagonize indoxyl sulfate (IS)-induced endothelial cell apoptosis, *Apoptosis* 25 (2020) 92–104, <https://doi.org/10.1007/s10495-019-01582-4>.
- [56] L. Martinez, M.G. Rojas, M. Tabbara, S. Pereira-Simon, N. Santos Falcon, M. A. Rauf, et al., The transcriptomics of the human vein transformation after arteriovenous fistula anastomosis uncovers layer-specific remodeling and hallmarks of maturation failure, *Kidney Int Rep.* 8 (2023) 837–850, <https://doi.org/10.1016/j.ekir.2023.01.008>.
- [57] J.L. Rukov, E. Gravesen, M.L. Mace, J. Hofman-Bang, J. Vinther, C.B. Andersen, et al., Effect of chronic uremia on the transcriptional profile of the calcified aorta analyzed by RNA sequencing, *Am. J. Physiol. Ren. Physiol.* 310 (2016) F477–F491, <https://doi.org/10.1152/ajprenal.00472.2015>.
- [58] L. Nguyen, E. Shubbar, M. Jernäs, I. Nookaew, J. Lundgren, B. Olsson, et al., Adenine-induced chronic renal failure in rats decreases aortic relaxation rate and alters expression of proteins involved in vascular smooth muscle calcium handling, *Acta Physiol (Oxford)* 218 (2016) 250–264, <https://doi.org/10.1111/apha.12724>.
- [59] S. Owada, S. Goto, K. Bannai, H. Hayashi, F. Nishijima, T. Niwa, Indoxyl sulfate reduces superoxide scavenging activity in the kidneys of normal and uremic rats, *Am. J. Nephrol.* 28 (2008) 446–454, <https://doi.org/10.1159/000112823>.
- [60] S. Roumeliotis, F. Mallamaci, C. Zoccali, Endothelial dysfunction in chronic kidney disease, from biology to clinical outcomes: a 2020 update, *J. Clin. Med.* 9 (2020), <https://doi.org/10.3390/jcm9082359>.
- [61] M. Cozzolino, M. Mangano, A. Stucchi, P. Ciceri, F. Conte, A. Galassi, Cardiovascular disease in dialysis patients, *Nephrol. Dial. Transplant.* 33 (2018) iii28–iii34, <https://doi.org/10.1093/ndt/gfy174>.
- [62] E. Devine, D.H. Krieter, M. Rütth, J. Jankovski, H.D. Lemke, Binding affinity and capacity for the uremic toxin indoxyl sulfate, *Toxins (Basel)* 6 (2014) 416–429, <https://doi.org/10.3390/toxins6020416>.
- [63] E. Mezzaroma, A. Abbate, S. Toldo, NLRP3 Inflammasome inhibitors in cardiovascular diseases, *Molecules* 26 (2021), <https://doi.org/10.3390/molecules26040976>.
- [64] C.L. Mayer, C.S. Parello, B.C. Lee, K. Itagaki, S. Kurosawa, D.J. Stearns-Kurosawa, Pro-coagulant endothelial dysfunction results from EHEC Shiga toxins and host damage-associated molecular patterns, *Front. Immunol.* 6 (2015) 155, <https://doi.org/10.3389/fimmu.2015.00155>.
- [65] M. Diaz-Ricart, S. Torramade-Moix, G. Pascual, M. Palomo, A.B. Moreno-Castaño, J. Martinez-Sanchez, et al., Endothelial damage, inflammation and immunity in chronic kidney disease, *Toxins (Basel)* 12 (2020), <https://doi.org/10.3390/toxins12060361>.
- [66] Y. Sun, C. Johnson, J. Zhou, L. Wang, Y.F. Li, Y. Lu, et al., Uremic toxins are conditional danger- or homeostasis-associated molecular patterns, *Front Biosci (Landmark Ed)* 23 (2018) 348–387, <https://doi.org/10.2741/4595>.